LBNL-45363, CBP Note 333

BEAM-BEAM SIMULATIONS FOR SEPARATED BEAMS*

Miguel A. Furman,† Center for Beam Physics, LBNL, Berkeley, CA 94720

Abstract

We present beam-beam simulation results from a strong-strong gaussian code for separated beams for the LHC and RHIC. The frequency spectrum produced by the beam-beam collisions is readily obtained and offers a good opportunity for experimental comparisons. Although our results for the emittance blowup are preliminary, we conclude that, for nominal parameter values, there is no significant difference between separated beams and center-on-center collisions.

1 INTRODUCTION AND SUMMARY.

In this note we present first results for beam-beam simulations for the LHC and RHIC with separated beams. There are two main motivations for these kind of simulations: (a) to assess undesirable effects from LBNL's sweeping luminosity monitoring scheme for the LHC [1], and (b) to assess undesirable effects form the process of bringing initially-separated beams into collision. In addition, we want to simulate conditions that might be testable at RHIC in order to test our understanding of strong-strong beam-beam dynamics in hadron colliders.

For the cases presented here, we have not found any indications of adverse effects for nominal parameter values. However, these simulations have been run for a maximum of 10^5 turns, which amount to only a brief interval of real accelerator time, so our conclusions are subject to change upon more detailed scrutiny.

The results presented here were obtained with a three-dimensional strong-strong gaussian code whose features are described below. This investigation represents a direct extension of the work by Krishnagopal [2], and Zorzano and Zimmermann [3].

2 SIMULATIONS.

2.1 Code features.

Our code is both an extension and a simplification of the code TRS [4]. It is a strong-strong simulation code in which the two colliding bunches are represented by a given number of macroparticles that are initially distributed gaussianly in 6-dimensional phase space. The beam and ring parameters for the two rings are fully independent. The heart of the code is the beam-beam module: at every turn, just before the beam-beam collision, the centers $\bar{x}$ and $\bar{y}$, and rms sizes σ_x and σ_y of the two distributions are computed from the macroparticle distributions, and these four dynamical quantities are fed into the Bassetti-Erskine [5] formula for the field of a relativistic gaussian distribution. The electromagnetic kick is computed from this expression and applied to each particle of the opposing beam. Then the role of the two beams is reversed before proceeding. Finite bunch-length effects are taken into account by slicing the bunch longitudinally; each such slice acts as a kick on the particle as it goes through the kicking bunch. A weak-strong mode is available as an option controlled by an input switch.

After the beam-beam kick, the beams are transported along the rings by a the action of a linear Courant-Snyder one-turn map that depends on the machine tunes and beta functions at the interaction point. A synchrotron rotation is performed on the longitudinal coordinates. Radiation damping and quantum excitation are applied once per turn by the action of a localized kick.

Our code can also describe beam-beam collision with separated beams by means of an input-specified closed-orbit displacement. This displacement can be static or time-dependent, and can be independently specified for either (or both) of the two beams. In addition, the code can optionally simulate a beam feedback element whose action is to shift the transverse position of the macroparticles so that their centroid is brought back to the specified closed orbit at every turn. Finally, the code can describe beams of various particle species, namely e^+, e^-, μ^+, μ^-, p, $\bar{p}$ and Au^{79+} ions in any desired combination. An extension to any other kind of ion is straightforward.

The code has, at present, several simplifications in the modeling of the collider. In particular, the beam-beam collisions have zero crossing angle; there is only one bunch per beam, so that there are no parasitic collisions; there is only one interaction point in the ring. These simplifications will be removed in future versions.

An intrinsic deficiency of the soft-gaussian approach is the introduction of an inconsistency in the calculation: although the actual macroparticle distribution deviates from the gaussian shape as time evolves, the beam-beam kick is always computed under the assumption of a gaussian shape. This inconsistency is, in principle, more serious for hadron simulations than for e^+e^- simulations, since

* Work supported by the US Department of Energy under contract no. DE-AC03-76SF00098. Presented at the US-LHC Collaboration mtg., BNL, Feb. 22–23, 2000; to be published in the proceedings.

† mafurman@lbl.gov

the damping times are typically much larger than typical simulation runs in the former case than in the latter. However, for short runs and weak beam-beam parameters, as in the examples presented here, we have checked that the distribution does not deviate significantly from the gaussian shape, and hence this inconsistency is not serious. The question remains, however, whether the gaussian shape is a good approximation to the actual particle distribution expected (or realized) in hadron colliders, particularly after long times following injection. We do not attempt to answer this question here. However, we intend to shed some light on this issue in the future by allowing the code to use distributions other than gaussian.

2.2 Simulation conditions.

As mentioned above, in all results in this note the crossing angle is zero, there is only one bunch per beam (no parasitic collisions), and there is only one interaction point in the ring. The damping time for the LHC at 7 TeV is 10^9 turns, and is larger for RHIC with Au^{79+} ions at 100 GeV/nucleon. Since our runs are for at most 10^5 turns, we have turned off radiation damping and quantum excitation in the code, which amounts to setting the damping time to ∞. The feedback is turned off. In all cases we use 10000 macroparticles per bunch. Other parameters are listed in Tables 1 and 2.

3 RESULTS.

3.1 Results for the LHC.

Nominal collision conditions. For reference we present first the results for nominal conditions, with parameters as specified in Table 1 and the beams colliding center-on-center. As seen in Fig. 1, the beam blowup is insignificant over 10^5 turns, and the rms sizes show the expected statistical fluctuations of order $M^{-1/2} = 1\%$ where M is the number of macroparticles.

Table 1: Selected LHC parameters [6].

Beam energy parameter, γ	7460.52
Protons per bunch, N	1.05×10^{11}
Beta-function at the IP, β^* [m]	0.5
RMS spot size at the IP, σ_0 [μm]	15.9
Nominal beam-beam parameter, ξ	-0.0034
Tunes, (ν_x, ν_y)	(0.31, 0.32)
RMS bunch length, σ_z [m]	0.077
Synchrotron tune, ν_s	0.0021

Fig. 2 shows the absolute value of the spectra of the sum and difference of the beam centroids. The coherent modes are clearly seen, with the σ modes at the lattice tunes. The π modes are downshifted from the σ modes by $\sim 1.1\xi$.

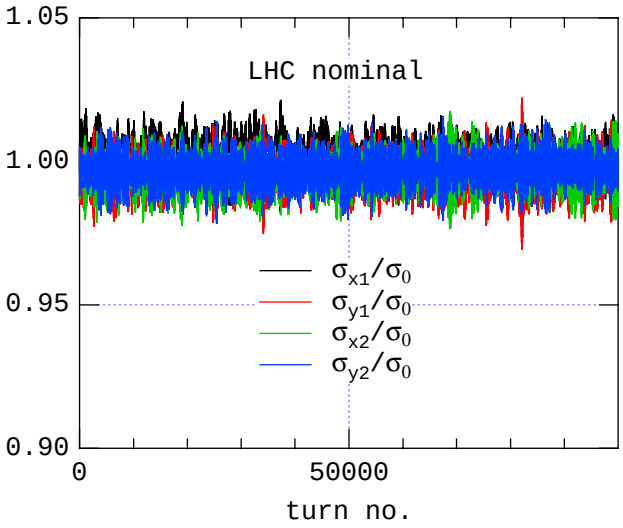

Figure 1: The rms beam sizes for nominal collisions.

The incoherent spectrum lies in between the two coherent modes.

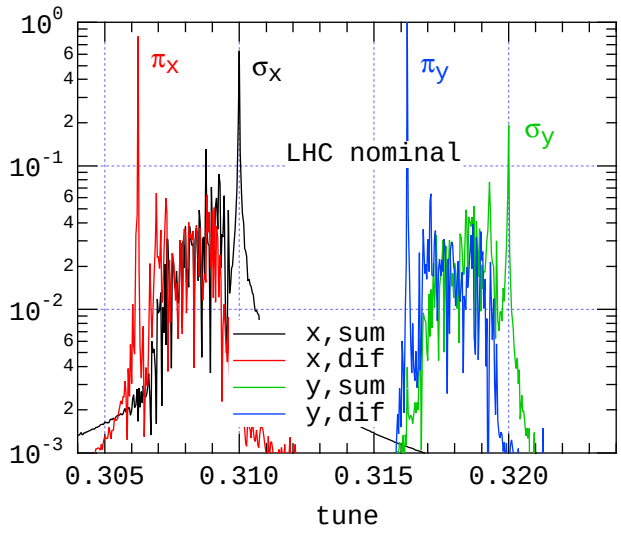

Figure 2: The beam-beam tune spectra during nominal collisions. The four traces are the absolute value of the spectra of the sum and difference of the beam centroids. The normalization is such that the highest peak among the four traces is arbitrarily set to unity; the relative heights of the traces are meaningful. Only the first 25000 turns were used in the computation.

Sweeping one beam about the other. In the luminosity monitoring scheme being developed at LBNL for the LHC one beam is deliberately swept in a circle about the other, which remains fixed. This sweeping is achieved by an appropriate time-dependent closed orbit bump spanning the IP. As a first test, we have chosen here a sweeping radius of $0.6\sigma_0$ for beam #2 while bunch #1 remains static and is offset by $0.2\sigma_0$ from the nominal IP at 45° relative to

the horizontal axis. The luminosity per collision is shown in Fig. 3, showing the characteristic fluctuations due to the off-center collisions with a period of 1000 turns, which is our chosen sweeping period. In practice, this is the signal that will be used to optimize the luminosity, although the period will be $\gg 1000$ turns. The rms beam sizes (Fig. 4) do not show significant differences with the nominal conditions (Fig. 1). Fig. 5 shows the beam centroid spectra; comparing with the nominal case (Fig. 2) one sees that the $\sigma - \pi$ tune split is smaller during the sweeping operation owing to the lower effective beam-beam parameter. The difference spectra also show sidebands of the π modes separated by 0.001, corresponding to the sweeping tune.

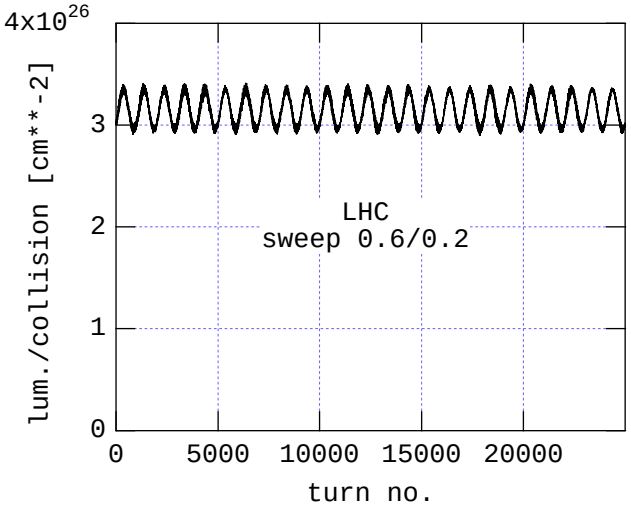

Figure 3: The luminosity per collision when bunch #2 sweeps about the nominal IP with a radius $0.6\sigma_0$ and a period of 1000 turns while bunch #1 remains static and is offset by $0.2\sigma_0$ from the nominal IP.

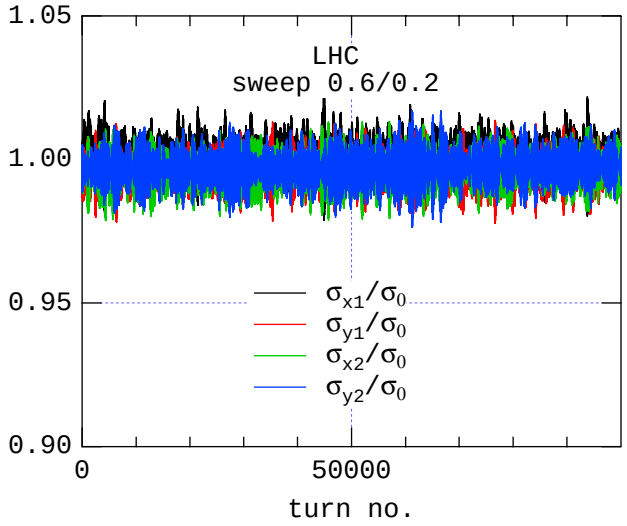

Figure 4: The rms beam sizes during the sweeping process.

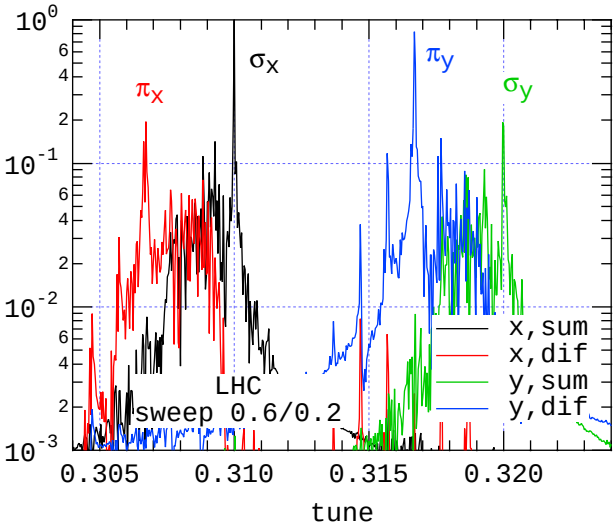

Figure 5: The beam-beam tune spectra during the sweeping process.

Statically offset collisions. We have also tested to see if constantly-separated beams are more sensitive to beam blowup than beams colliding head-on. Fig. 6 shows the rms beam sizes for the case in which beam #2 is displaced vertically from beam #1 by $3\sigma_0$ and is held fixed in this position. Comparing with the nominal case (Fig. 1), there is no significant difference. Fig. 7 shows the beam centroid spectra. Comparing with the nominal case, Fig. 2, there is an important qualitative difference: the π_y coherent mode is *upshifted* from the σ_y mode rather than downshifted. This change is due to the fact that the slope of the beam-beam force at a separation of 3σ has the opposite sign from the slope near the origin. In addition, of course, the $\sigma_x - \pi_x$ tune split is smaller than in the nominal case owing to the smaller effective beam-beam parameter.

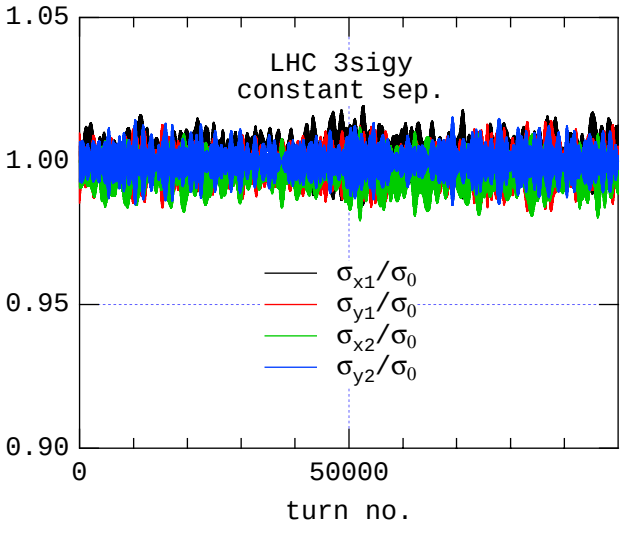

Figure 6: The rms beam sizes when beam #2 is displaced vertically from beam #1 by $3\sigma_0$.

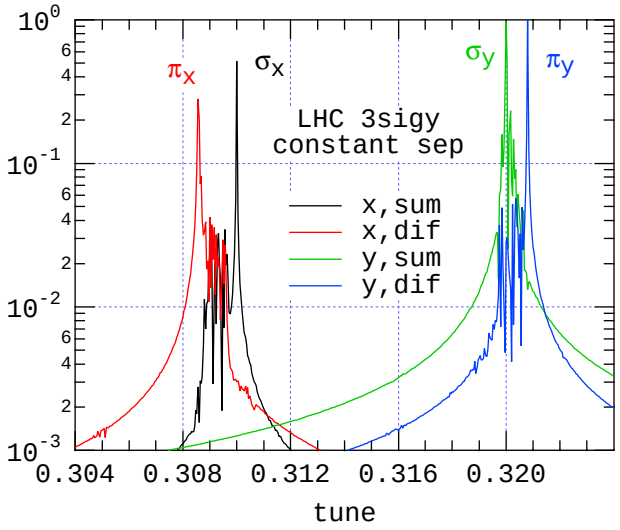

Figure 7: The beam centroid spectra in case that beam #2 is displaced vertically from beam #1 by $3\sigma_0$. Notice that the π_y coherent mode is upshifted from the σ_y mode.

Closed-orbit squeeze. We have also tested to see if any undesirable effects appear when the beams are brought transversely into collision following the end of the acceleration ramp. For this purpose we assume that the closed orbit of beam #2 starts outs vertically displaced from the nominal IP by $3\sigma_0$ and is linearly brought down to the nominal IP over a time interval of 25000 turns, while beam #1 is held fixed at the nominal IP. We ran the simulation for an additional 5000 turns for a total of 30000 turns. Fig. 8 shows the normalized beam centers, $\bar{x}_i/\sigma_0$ and $\bar{y}_i/\sigma_0$ as a function of time, for $i = 1, 2$. Fig. 9 shows the rms beam sizes, and Fig. 10 shows the luminosity per collision during this process, exhibiting the characteristic gaussian shape as the beam overlap increases.

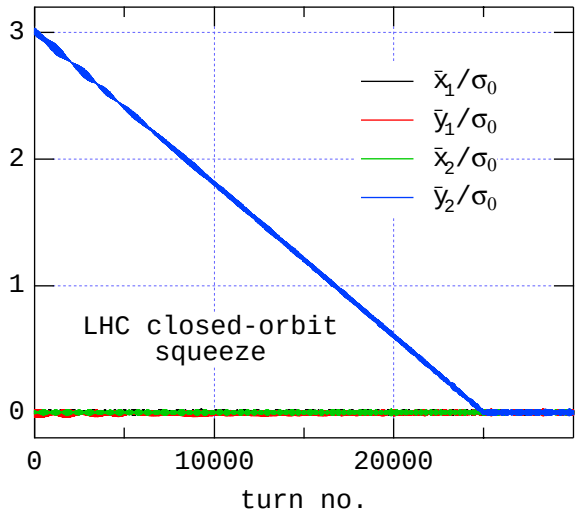

Figure 8: The normalized beam centers as a function of time during a vertical closed-orbit squeeze.

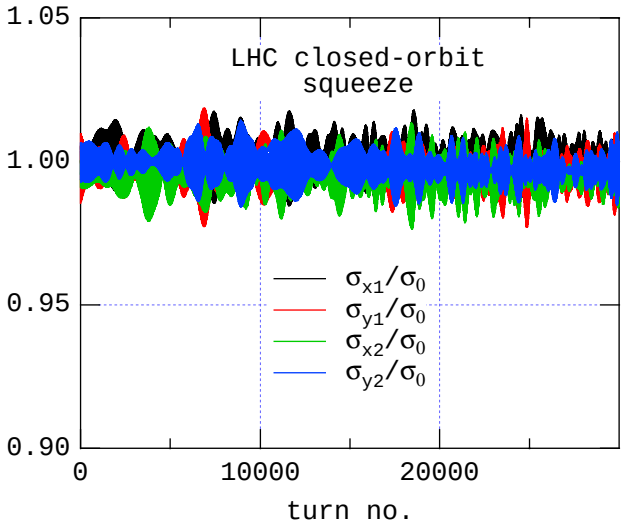

Figure 9: The rms beam sizes as a function of time during a vertical closed-orbit squeeze.

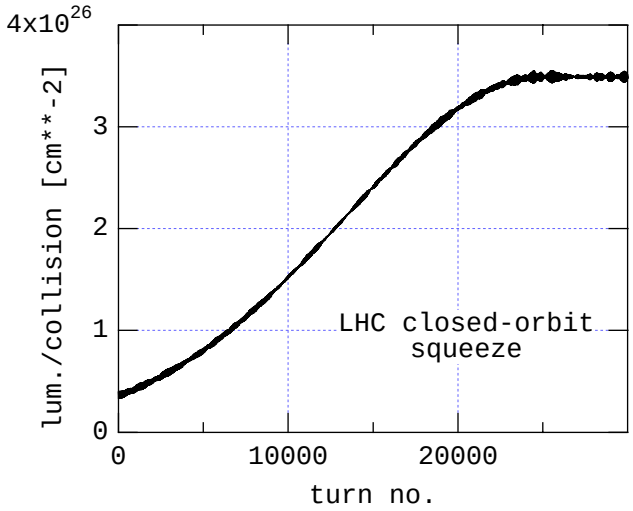

Figure 10: The luminosity per collision as a function of time during a vertical closed-orbit squeeze.

3.2 Results for RHIC.

Nominal collision conditions. Nominal conditions for RHIC are shown in Table 2. For these conditions, Fig. 11 shows the beam centroid spectra. As in the case of the LHC, the σ coherent modes are located at the ring tunes, and the π modes are downshifted from the σ modes by 1.1ξ.

Split tunes. We have run one case in which the tunes of the two rings are split by 0.005, so that all four tunes are different, $(\nu_{x1}\,, \nu_{y1}) = (0.190, 0.195)$ and $(\nu_{x2}\,, \nu_{y2}) = (0.180, 0.185)$. In this case, as shown in Fig. 12, all coherent modes have disappeared, as expected from the theory [8].

Table 2: Selected RHIC parameters [7].

Beam energy parameter, γ	106.5
Au^{79+} ions per bunch, N	1×10^9
Beta-function at the IP, β^* [m]	10
RMS spot size at the IP, σ^* [μm]	396
Nominal beam-beam parameter, ξ	-0.0023
Tunes, (ν_x, ν_y)	(0.19, 0.18)
RMS bunch length, σ_z [m]	1
Synchrotron tune, ν_s	0.000745

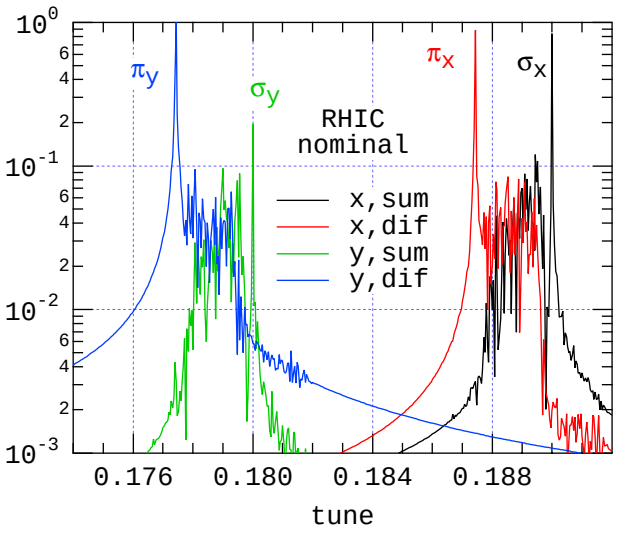

Figure 11: Beam centroid spectra for nominal collision conditions (Table 2).

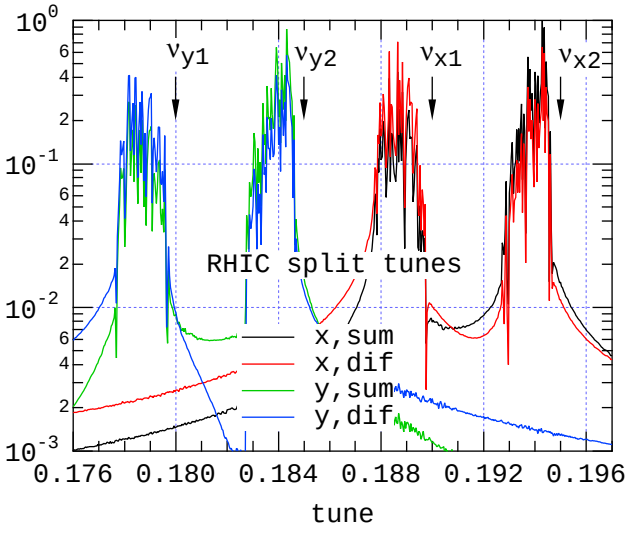

Figure 12: Beam centroid spectra for split tunes, indicated by the arrows. Other parameters are as specified in Table 2. Notice that all coherent modes have disappeared.

Semi-weak-strong case. By "semi-weak-strong" we simply mean that the number of particles per bunch is different in the two beams. Specifically, we choose $N_1 = 2 \times 10^9$, with other parameters as specified in Table 2. As seen in Fig. 13, the π modes have disappeared because they have shifted into the continuum of the spectrum and hence have Landau-damped, in agreement with theoretical expectations [8].

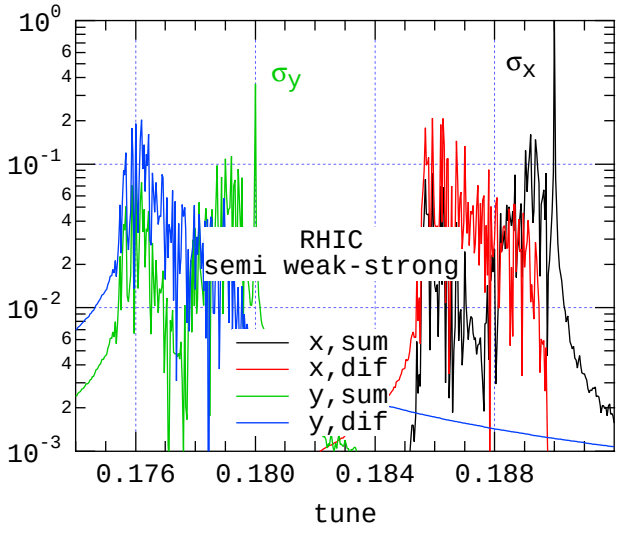

Figure 13: Beam centroid spectra for unequal bunch intensities: $N_1 = 2 \times 10^9$, $N_2 = 1 \times 10^9$. Other parameters are as specified in Table 2. Notice that the π modes have disappeared.

Weak-strong case. Finally, we present a simulation in the "weak-strong" mode that is only of mathematical interest. In this case beam #2 is represented by a mathematical gaussian lens rather than by a collection of macroparticles. Other than this, all parameters are as stated in Table 2; in particular, the number of particles per bunch and the tunes are the same for the two beams. In this case both coherent modes have disappeared, and the spectrum only shows the incoherent part. The sum and difference spectra coincide exactly, since beam #2 is static.

4 DISCUSSION.

The appearance of coherent dipole beam-beam modes is perhaps the cleanest manifestation of the beam-beam interaction in strong-strong mode and offers the possibility of simple and meaningful comparisons with experiment. Three examples of such measurements are: (1) the tune shift of the π mode as a function of beam-beam separation; (2) the disappearance of the coherent modes as the tunes of the two rings move away from each other; and (3) the disappearance of the π modes as the bunch intensities of the two beams become sufficiently different. The thresholds and magnitudes of these effects can be readily computed by simulations, as our samples show. Of course, one has

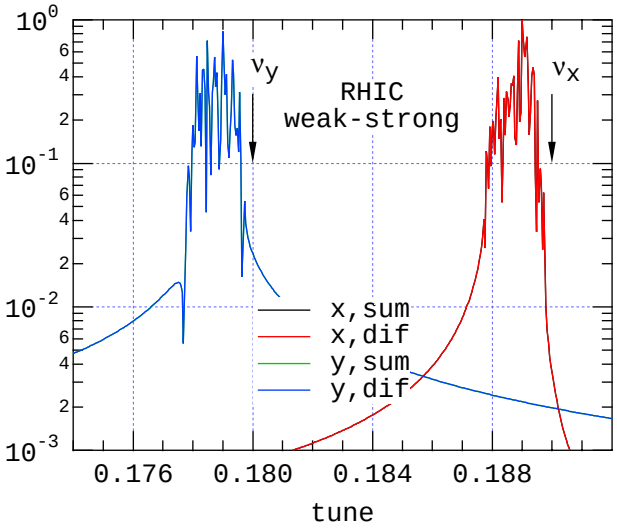

Figure 14: Spectrum for a weak-strong simulation in which beam #2 is represented by a static gaussian lens. All parameters are as shown in Table 2. The sum and difference spectra coincide exactly. Note the absence of coherent modes.

to make sure that the tune spread from lattice nonlinearities is small enough, otherwise the coherent modes might be Landau-damped. Obviously this issue requires further detailed study.

For a few selected cases we have verified that our results are in excellent agreement with those in Ref. 3, lending support to the validity of the two codes.

The coherent beam-beam renormalization factor $|(\nu_\pi - \nu_\sigma)/\xi|$ has the value 1.1 in our calculations, which appears to be $\sim 10\%$ smaller than analytic estimates [9, 8]. We do not know if this difference is significant.

For the cases with separated beams (static separation, closed-orbit squeeze, and beam sweeping), our results do not show noticeable detrimental effects such as emittance blowup. Of course our conclusions are based on relatively short runs, and may change upon further examination. Nevertheless, it is encouraging that there is no significant difference with the case of nominal, center-on-center, collisions.

Since σ_z/β^* is small for both machines, we have used in all cases shown here the impulse approximation (finite-bunch-length effects represented by a single slice) for the beam-beam collision. We have verified that this is a valid approximation by running sample cases with five slices, which show insignificant differences with the single-slice cases. The advantage of the single-slice calculations is computational speed, since the CPU time is proportional to the number of slices used in the beam-beam collision. Although synchrotron motion leads, even in the impulse approximation, to synchrobetatron coupling, the effects from this coupling are very weak in the cases reported here owing to the smallness of ν_s and σ_z/β^*. As a result, it is legitimate to ignore the longitudinal motion by setting $\nu_s = 0$, although we have not bothered to do so. The implementation of a crossing angle in our calculations might introduce more significant synchrobetatron coupling effects.

For 10000 macroparticles per beam in strong-strong mode and a linear lattice map, our runs take ~ 5600 CPU seconds to run for 25000 turns on a Cray SV1 computer at NERSC. In this regime the computer speed is limited by the calculation of the beam-beam force, and overall CPU time scales with the product (number of turns)$\times$(number of slices)$\times$(number of macroparticles). If we turn on the radiation damping and quantum excitation elements, computer speed is only slightly lower.

We have initiated sensitivity studies with respect to two parameters that are directly relevant to the cost (in terms of CPU time) and reliability of our simulations, namely: the number of macroparticles per bunch, and the length of the simulation. The beam centroid spectra is quite insensitive to these two parameters: even 100 macroparticles per bunch running for 1000 turns yield very accurately the tunes of the coherent modes. On the other hand, beam blowup is not given reliably when one uses few macroparticles.

As mentioned above, an intrinsic limitation of our code is the gaussian approximation. Although the initial distribution in our simulations is, by construction, gaussian, this shape cannot in principle persist for long times owing to the nonlinearities of the beam-beam force. For the nominal LHC beam-beam parameter value we have verified that the deviations from the gaussian shape of the distributions are insignificant up to 10^5 turns, although these deviations become clear (though still a few percent) in sample runs for bunch intensities 10 times the nominal value. Furthermore, in a real hadron collider, the initial particle distribution is sensitive to the injection process, and is unlikely to be exactly gaussian. We plan to augment our simulation code by allowing shapes other than gaussian (but still of a prescribed functional form), and determining the effect of the change on the beam centroid spectra. We also plan to optimize the PIC code CBI [10], which does not make any assumption about the shape of the distribution, by adapting it to a parallel computer.

The gaussian approximation (or, indeed, any approximation of a specific functional form) leads to purely numerical beam blowup that might mask physical blowup effects due to the nonlinearities of the forces. Fig. 15 shows the result for the rms beam sizes for the LHC for bunch intensities 10 times the nominal value. There is an approximately linear increase in beam size whose slope we may call $\dot{\sigma}$. By repeating this calculation for 100 and 1000 macroparticles, we have found the empirical scaling law $\dot{\sigma} \propto M^{-p}$ where M is the number of macroparticles and the scaling exponent is $p \simeq 0.7 - 0.8$. Further investigations are planned, particularly the dependence on tune and on beam separation.

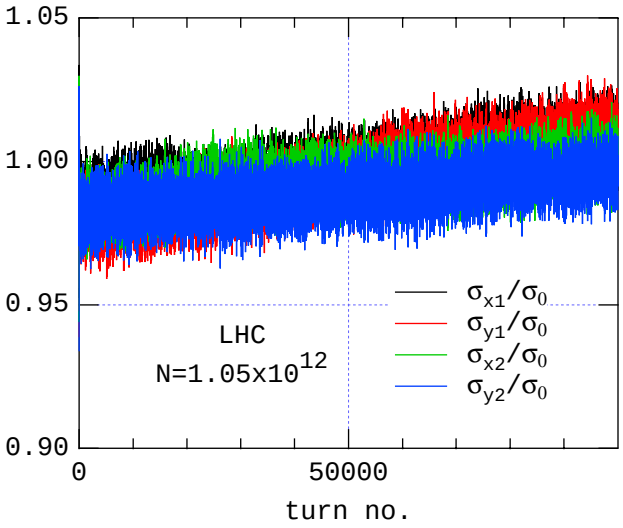

Figure 15: The rms beam sizes for LHC collisions for bunch intensities 10 times the nominal value.

5 ACKNOWLEDGMENTS.

I am grateful to F. Zimmermann, M. P. Zorzano, W. Turner and S. Krishnagopal for discussions and to NESRC for supercomputer support.

6 REFERENCES

[1] W. Turner, these proceedings.

[2] S. Krishnagopal, M. A. Furman and W. C. Turner, "Studies of the Beam-Beam Interaction for the LHC," Proc. PAC99, New York City, March 29-April 2, 1999, p. 1674; S. Krishnagopal, "Collective Beam-Beam Effects in the LHC," Proc. Workshop on Beam-Beam Effects in Large Hadron Colliders LHC99, April 12–17, 1999, CERN-SL-99-039 AP, p. 52.

[3] M. P. Zorzano and F. Zimmermann, "Coherent Beam-Beam Oscillations at the LHC," LHC-PR-314, 2 November 1999.

[4] J. L. Tennyson, undocumented code "TRS," 1989.

[5] M. Bassetti and G. A. Erskine, "Closed Expression for the Electric Field of a Two-Dimensional Gaussian Charge," CERN-ISR-TH/80-06.

[6] "The Large Hadron Collider: Conceptual Design," CERN/AC/95-05(LHC), 20 October 1995.

[7] "RHIC Design Manual," http://www.agsrhichome.bnl.gov/NT-share/rhicdm/00_toc1i.htm.

[8] Y. Alexahin, "Eigenmodes of Coherent Oscillations in Colliding Beams," Proc. Workshop on Beam-Beam Effects in Large Hadron Colliders LHC99, April 12–17, 1999, CERN-SL-99-039 AP, p. 41, and references contained therein.

[9] R. E. Meller and R. H. Siemann, "Coherent Normal Modes of Colliding Beams," IEEE Trans. Nucl. Sci. **NS-28** No. 3, 2431 (1981); K. Yokoya, Y. Funakoshi, E. Kikutani, H. Koiso and J. Urakawa, "Tune Shift of Coherent Beam-Beam Oscillations," KEK Preprint 89-14; K. Yokoya and H. Koiso, Part. Accel. **27**, pp. 181–186 (1990).

[10] S. Krishnagopal, "Luminosity-Limiting Coherent Phenomena in Electron-Positron Colliders," Phys. Rev. Lett. **76**, pp. 235–238 (1996); "Energy Transparency and Symmetries in the Beam-Beam Interaction," PRST-AB **3**, 024401 (2000).